Role of quantum paths in generation of attosecond pulses

M R Sami and A Shahbaz†

Department of Physics, Government College University, P.O. Box 54000 Lahore, Pakistan

(Received 13 March 2020; revised manuscript received 3 May 2020; accepted manuscript online 18 June 2020)

We investigate the role of core potential in high ionization potential systems on high harmonic generation (HHG) spectra and obtain attosecond pulses. In our scheme, we use a standard soft core potential to model high ionization potential systems and irradiated these systems with fixed laser parameters. We observe the role of these systems on all the three steps involved in HHG process including ionization, propagation and recombination. In our study, the results illustrate that for high ionization potential systems, the HHG process is more sensitive to the ionization probability compared to the recombination amplitude. We also observe that due to the stronger core potential, small oscillations of the electrons during the propagation do not contribute to the HHG spectrum, which implies the dominance of only long quantum paths in the HHG spectrum. Our results, for attosecond pulse generation, show that long quantum path electrons are responsible for the supercontinuum region near the cutoff, which is suitable for the extraction of a single attosecond pulse in this region.

Keywords: high-order harmonic generation, attosecond pulses, quantum paths, strong nuclear potential

PACS: 42.65.ky, 42.65.Re, 02.60.Cb **DOI:** 10.1088/1674-1056/ab9deb

1. Introduction

Understanding of molecular dynamics, which involves structural changes with time during chemical bonding, is now possible using femtosecond laser pulses.[1–3] The possibility of time-resolved observations of dynamical systems on timescales of femtoseconds has opened up an opportunity to look into ultrafast phenomena in real time. New methods of time-resolved spectroscopy have already crossed the barrier of femtosecond time regime and have now entered the domain of attosecond timescales, which can resolve the motion of the electrons at the atomic level.[4–8] In particular, isolated single attosecond pulses (SAPs) have gained interest due to their applications in typical pump-probe experiments,[9–11] where, in principle, one requires attosecond pump and attosecond probe pulses. In recent years, a lot of efforts have been made to meet the challenges of generating coherent ultrashort pulses through different processes. In this way, high harmonic generation (HHG)[12,13] is one of the potential candidates for generating SAPs and has been used extensively for this purpose.[14–18]

HHG is a nonlinear process and well described by the semiclassical three step model (TSM),[19,20] which involves the extraction of the electron from the atom by using an incident laser field of a suitable frequency. A free electron in the influence of an external field accelerates away from the core and finally when the laser field changes its direction, it may recombine with the core by emitting a photon of energy that is a multiple of the energy of the incident photon. The spectrum obtained via this process is limited by the cutoff energy law $E_c = I_p + 3.17U_p$, where I_p is the ionization potential energy of the system and U_p is the ponderomotive potential. The HHG spectrum has some distinct features. Firstly, there is an exponential decrease in the intensity of the first few low order harmonics, which is due to the contribution of the unabsorbed photons. This is followed by a plateau region, where all the harmonics have comparable intensity. Finally, the HHG spectrum terminates with a sharp cutoff.

In the last few years, extensive efforts have been made both experimentally and theoretically to enhance the efficiency of the emitted photons and broaden the plateau region of the HHG spectrum in order to generate ultrashort light pulses in the extreme ultraviolet region.[21–24] The common way of broadening the HHG spectrum is to increase the amplitude or the wavelength of the incident laser field. However, these parameters can cause depletion of the ground state, which affects the conversion efficiency. While an increasing number of cycles of the incident laser field can increase the intensity of the emitted harmonics, this scheme generally decreases the probability of getting an SAP. Therefore, various other methods have been employed. For instance, short incident laser pulses using envelope functions are used to generate an SAP. Two or multicolor fields are also used to break the symmetry of the incident laser fields, which not only increases the cutoff but also helps to generate an SAP. The carrier-envelope phase (CEP) and the delay between the two-color laser fields are also noteworthy parameters to generate an SAP. In fact, in the last decade, several methods for tailoring the incident laser field have been successfully implemented in order to optimize the attosecond pulses.[25,26] A different approach is to use high ionization potential systems, which plays a significant role in broadening the HHG spectrum, which are routinely generated across several laboratories in the world.[27–34] In fact, these systems have been used before to enhance the

†Corresponding author. E-mail: atif-shahbaz@gcu.edu.pk

cutoff position.[35,36] However, due to the strong binding potential, these systems decrease the ionization rate, which decreases the intensity of the emitted harmonics. This problem may be handled using an incident laser field of higher intensity because these systems can withstand higher intensities without depletion of their ground states due to their stronger binding potential.

In addition to an intense and broadened HHG spectrum, in-phase harmonics near the cutoff region can be useful to generate SAPs. In this regard, quantum paths[37–39] show a significant contribution to generate SAPs from the cutoff harmonics because these paths can be optimized to generate a supercontinuum region (structure with more in-phase harmonics). Due to different emission times, harmonics are not emitted in-phase and an interference structure is obtained due to the contribution of two (long and short) quantum paths. From the perspective of SAP generation, it is known that a cutoff region consisting mainly of a single quantum path is more beneficial.

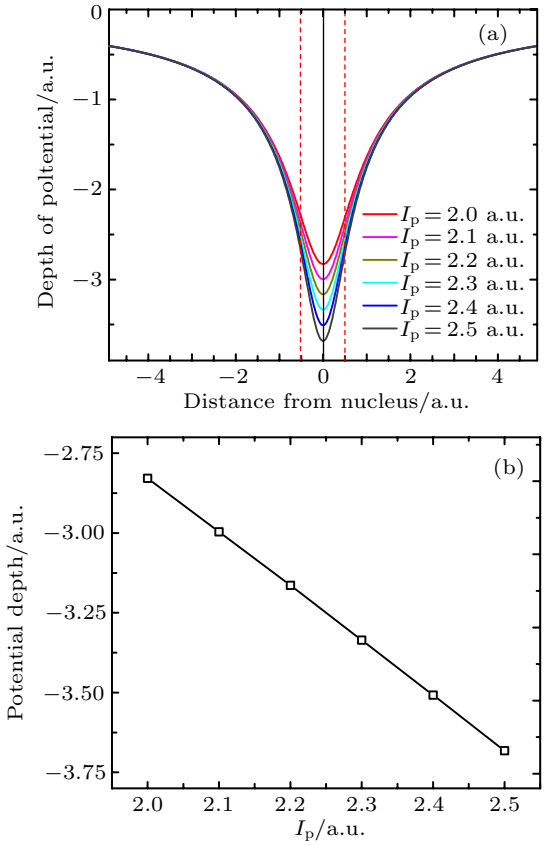

Fig. 1. (a) Potential as a function of the distance from the nucleus and (b) the corresponding potential depths as a function of I_p.

Generally, optimization of the quantum paths is associated with the incident laser fields. In this paper, we find the impact of system potentials on the quantum paths for fixed laser parameters. For systems with high ionization potential energies such as hydrogen-like ions, a single orbiting electron comes closer to the nucleus, where the nucleus features can affect the ionization/recombination times during the HHG process. For this purpose, we increase I_p and see the effects of the nucleus on all the three steps involved in the TSM. We discuss the role of recombination amplitudes and ionization probabilities on the HHG spectra that are obtained using high ionization potential systems. Further, using time-frequency analysis, we discuss the impact of stronger nuclear potential on quantum paths and attosecond pulses.

2. Theoretical aspects

To investigate the HHG spectrum and attosecond pulses, the time-dependent Schrödinger equation (TDSE) is numerically solved for model high ionization potential systems. Solutions are obtained within the dipole approximation using the Crank Nicholson scheme in one dimension (1D). The Schrödinger equation of the classical Hamiltonian can be found by replacing the observables with the corresponding operators via using the principle of first quantisation[40–42] to obtain the 'semiclassical' Schrödinger equation, given as (atomic units are used throughout in this paper unless stated otherwise)

$$\mathrm{i}\frac{\partial}{\partial t}\psi(x,t) = \Big[-\frac{1}{2}\frac{\partial^2}{\partial x^2} + V(x) - xE(t)\Big]\psi(x,t), \tag{1}$$

where $E(t)$ represents the driving linear field and expressed as

$$E(t) = E_0 f(t)\cos(\omega t), \tag{2}$$

where E_0 and ω are the peak amplitude and the frequency, respectively, while $f(t)$ is the Gaussian envelope function given as $f(t) = \exp[-4(\ln 2)t^2/\tau^2]$, and $V(x)$ models the high ionization potential systems[43] as

$$V(x) = -\frac{2}{\sqrt{x^2+a^2}}. \tag{3}$$

The Ehrenfest theorem[44] is used to calculate the time-dependent acceleration

$$a(t) = \Big\langle \psi(x,t)\Big|\frac{\partial V(x)}{\partial x} - E(t)\Big|\psi(x,t)\Big\rangle. \tag{4}$$

Fourier transformation of this time-dependent acceleration gives the HHG spectrum

$$P_A(\omega) = \Big|\frac{1}{2\pi}\int_0^T a(t)\,\mathrm{e}^{-\mathrm{i}\omega t}\,\mathrm{d}t\Big|^2. \tag{5}$$

Calculations for the recombination amplitude for softcore potentials in 1D[45] are carried out as

$$a_{reco}(k) = -\frac{1}{\sqrt{2\pi}}\int \mathrm{e}^{\mathrm{i}kx}\psi_0^* V'(x)\,\mathrm{d}x. \tag{6}$$

The time-dependent ionization probabilities are calculated as

$$p(t) = 1 - \sum_n \Big|\phi_n(x)|\psi(x,t)\Big|^2, \tag{7}$$

where $\phi_n(x)$ is the bound state wavefunction of high ionization potential systems. The electron wave packet density is calculated by

$$\rho(x,t) = \Big|\psi(x,t)\Big|^2. \tag{8}$$

3. Results and discussion

In our simulations, we increase I_p to model a system with stronger nuclear potential by changing the soft parameter a (Eq. (3)) and observe the effects of these systems on the HHG spectrum and attosecond pulses. Values of I_p used with the corresponding 1D potentials are shown in Fig. 1(a), whereas the linear increase in the potential depths are plotted as a function of I_p in Fig. 1(b). We irradiate these systems by a fixed laser field, for which parameters are chosen to be 5 fs/800 nm with a field intensity of $I = 1.0 \times 10^{15}$ W/cm^2.

Figure 2 represents the HHG spectra obtained through numerical simulations using the single electron approximation (SEA) for the above-mentioned systems. This figure shows that the cutoff positions are extended from the 163rd harmonic order to the 175th harmonic order and these values are consistent with the values that are obtained using the cutoff energy law. The yield of the emitted harmonics decreases by one order of magnitude for each increment of 0.1 a.u. in the ionization potential energy of the system. Since the yield of the emitted harmonics is determined by all the three steps involved in the well-described three-step model, we perform different analyses to describe the involvement of each step in the HHG spectra for the model potential systems. For this, we start with the last step, that is, recombination, because it is sensitive to the cusp of a given potential. A deeper cusp gives a stronger recombination amplitude, which results in a better yield for the emitted harmonics for the same system.[45] Recombination amplitudes for all the potentials (given in Fig. 1(a)) are plotted as a function of kinetic energy in Fig. 3(a) and this figure shows, as expected, that recombination amplitudes become stronger with strengthening potentials, on the contrary there is a substantial decrease in the yield of the corresponding spectra (Fig. 2). The increase in I_p provides a stronger nuclear pull towards a single electron, which is due to the deeper potential because of each increment of 0.1 a.u. and this increase in depth results in stronger recombinations.

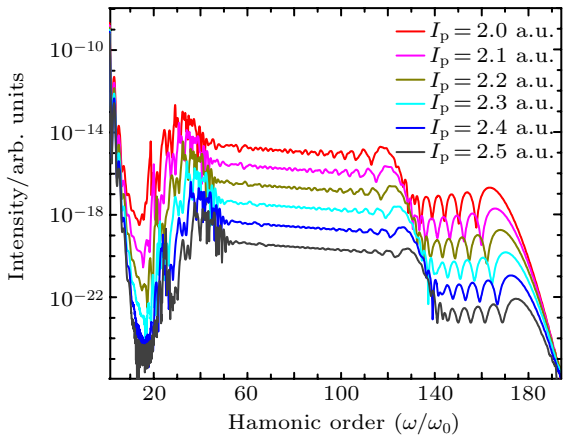

Fig. 2. Calculated HHG spectra through numerical simulation of 1D-TDSE, considering potentials given in Fig. 1.

While these model potentials provide stronger nuclear pull during recombination to complete the HHG process, the increment in the ionization potential energy of the system decreases the ability of the external laser field to initialize the HHG process. This is due to the fact that an increase in I_p affects the ionization probability in the presence of the incident laser field with a fixed set of parameters. In order to demonstrate this, we use the fact that $I_p = 2.0$ a.u. corresponds to helium ions, for which the Bohr radius is 0.5 a.u. and when we increase I_p, the Bohr radius for these systems reduces to the value less than 0.5 a.u. Hence, the height of the potential barrier grows and it becomes harder for the electron wavefunction to tunnel out with the same set of laser parameters. Therefore, this fact actually decreases the ionization probability for the electron wavefunction to tunnel through the potential barrier. For reference, calculated ionization probabilities are shown in Fig. 3(b). Clearly, this figure shows that the ionization probabilities decrease with the increase in I_p because the electron gets closer to the nucleus with the increase in I_p.

We also calculate electron wavepacket densities for systems having $I_p = 2.0$ a.u. and 2.5 a.u. and these densities are shown in Figs. 4(a) and 4(b). Analysis of these graphs shows that for high ionization potential systems, the electron

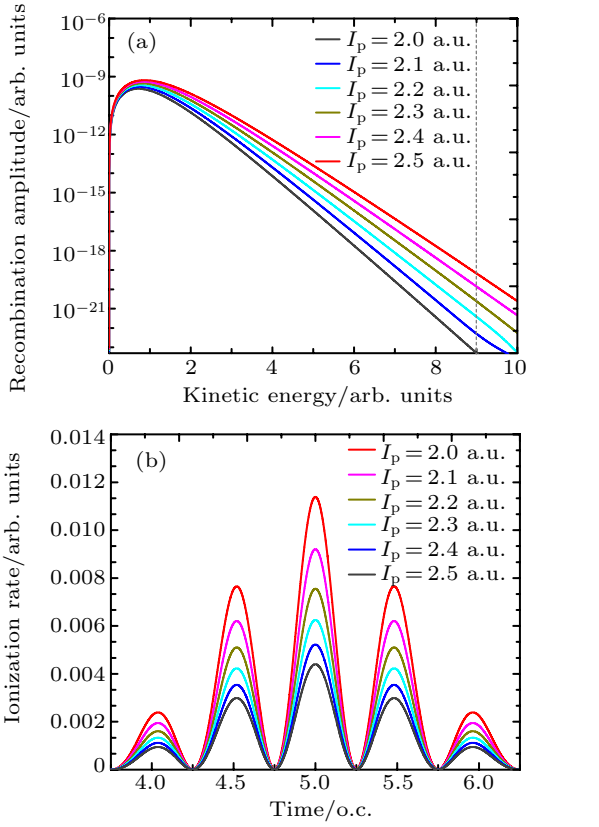

Fig. 3. (a) Recombination amplitudes for all potentials given in Fig. 1. (b) Calculated ionization probabilities corresponding to each system given in Fig. 1, when these are irradiated by an external electric field of fixed laser parameters.

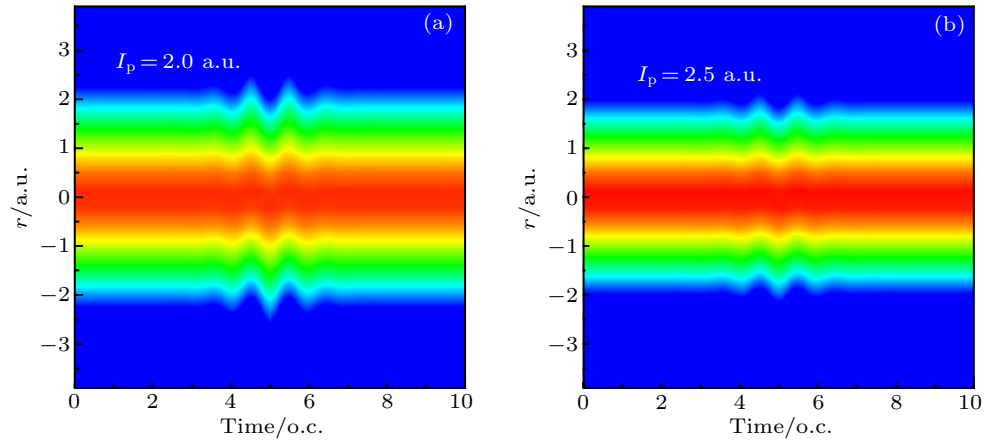

Fig. 4. Electron wavefunction density for systems having (a) $I_p = 2.0$ a.u. and (b) $I_p = 2.5$ a.u.

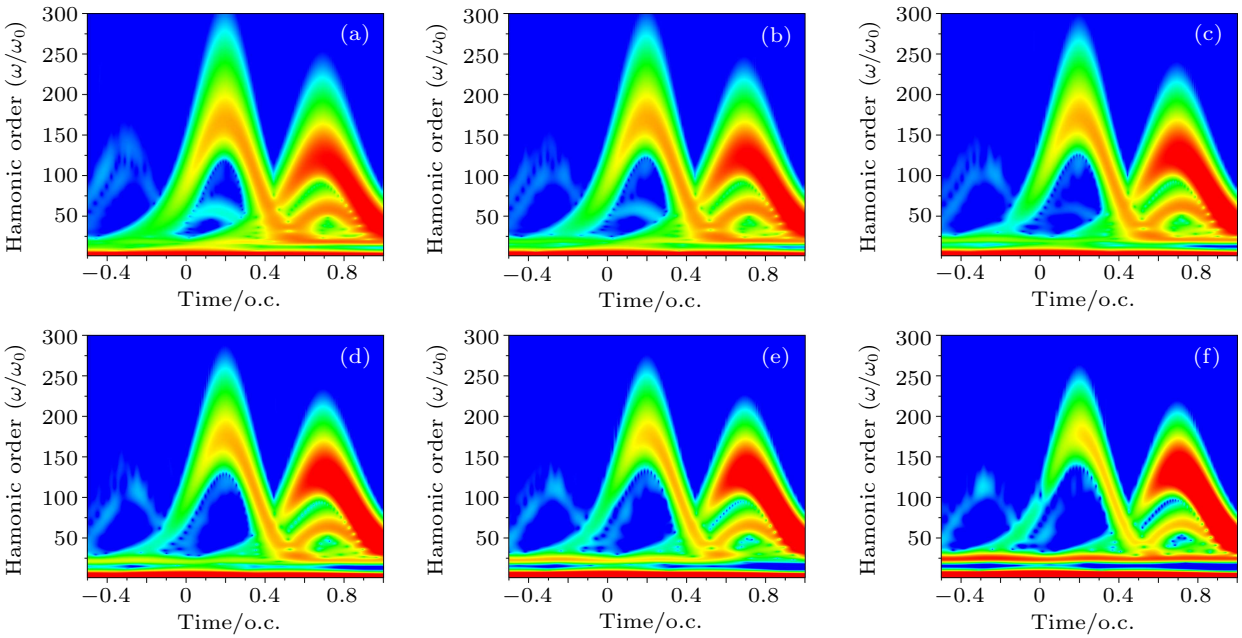

Fig. 5. Time-frequency distribution of the HHG spectra when model potentials given in Fig. 1 are exposed to a single 5 fs/800 nm laser field with a peak intensity of 1.0×10^{15} W/cm^2. Long and short quantum trajectories are calculated only for 1.5 cycles for a cosine-like pulse. These laser parameters are kept to be constant for each system, where (a) $I_p = 2.0$ a.u., (b) $I_p = 2.1$ a.u., (c) $I_p = 2.2$ a.u., (d) $I_p = 2.3$ a.u., (e) $I_p = 2.4$ a.u., (f) $I_p = 2.5$ a.u.

is mainly located around its core potential even for strong field strengths, whereas for an atomic system,[46] similar field strengths drive electron wavefunctions for longer distances or even cause depletion of the ground state. A decrease in the ionization probabilities and the extent of the electron wavefunction for high ionization potential systems causes a decrease in the intensity of the emitted harmonics. Thus, this reveals that for fixed laser parameters, the yield of the emitted harmonics is more sensitive to the ionization probability amplitude compared to the recombination amplitude.

Further, we perform a time-frequency analysis to observe the role of the stronger nuclear pull for high ionization potential systems during propagation in the external field along the quantum paths and these are shown in Figs. 5(a)–5(f). These graphs show that for $I_p = 2.0$ a.u., both short and long quantum paths contribute to the cutoff harmonics, but when we increase the ionization potential energy, the short quantum paths get reduced. The electrons that are created soon after the field crest and return between three-quarters of a period to one period later are known as long path electrons. However, there are also electrons that are created later and return earlier, which are known as short quantum path electrons. Because the spatial phase of the XUV radiation produced by the electrons from long and short quantum paths are different, the corresponding electric fields interfere in the far field. This interference can be constructive or destructive and one usually ends up with the short path contributions. Different gating techniques are used to separate the spatial paths in the far field of the produced radiation from long and short paths. Classically, we can say that due to the strong nuclear pull of high ionization potential systems, small oscillations of electrons do not contribute to the HHG process. Although the reduction of short

quantum paths decreases the intensity of the emitted harmonics, the dominance of single (long) quantum paths increases the probability of getting in-phase harmonics in the cutoff region. This produces a supercontinuum near the cutoff region, which is suitable to generate single isolated pulses from this region without any need of gating techniques.

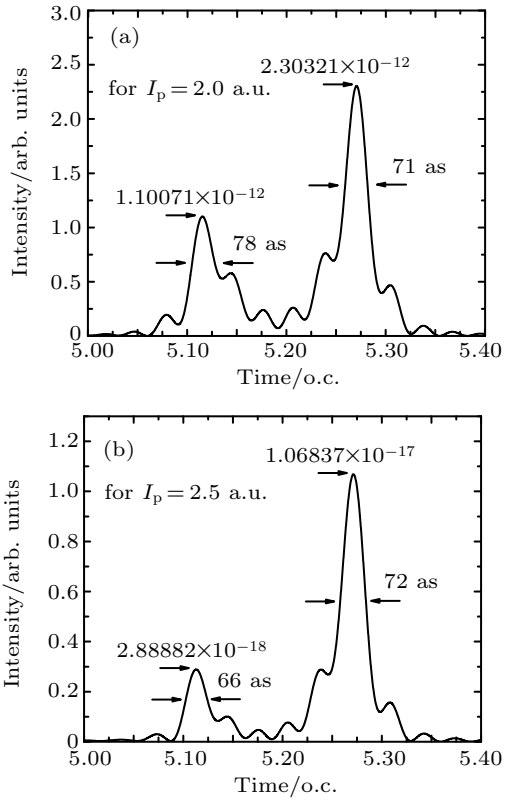

Fig. 6. (a) The temporal profile of the attosecond pulses by superposing harmonics from the 130th to 165th order for the system with $I_p = 2.0$ a.u. and (b) the temporal profile of the attosecond pulses by superposing harmonics from the 140th to 175th order for the system with $I_p = 2.5$ a.u.

Since quantum paths contribute significantly in attosecond pulse generation, we calculate attosecond pulses for systems having $I_p = 2.0$ a.u. and 2.5 a.u. These attosecond pulses are illustrated in Figs. 6(a) and 6(b). For $I_p = 2.0$ a.u., two attosecond pulses (78 as and 71 as) of comparable intensities are generated by superposing harmonics from the 130th to 165th order. However, for $I_p = 2.5$ a.u., two attosecond pulses (66 as and 72 as) are generated by superposing harmonics from the 140th to 175th order. In this case, the intensity of the 66 as pulse is decreased by one order of magnitude, compared to the 72 as pulse. This decrease in intensity in one of the two generated pulses is also due to the reduction of the short quantum paths, which is caused by stronger nuclear potential. For $I_p = 2.0$ a.u., both long and short quantum paths contribute to the cutoff harmonics. This contribution gives rise to the interference structure in the cutoff region. Therefore, the two attosecond pulses generated are of comparable intensities. For $I_p = 2.5$ a.u., only long quantum paths contribute to the cutoff harmonics. These long quantum paths produce more in-phase harmonics near the cutoff and hence decreases the intensity of one of the two pulses.

4. Conclusion

In summary, we theoretically investigate the effects of the core potential on the HHG spectrum and attosecond pulses, using model high ionization potential systems. The cutoff energy law suggests that the increase in the ionization potential energy of the system causes an extension in the HHG spectrum. However, this law does not accommodate the effect of the increase in I_p value on the efficiency of the emitted harmonics. The increment in the I_p gives a deeper cusp due to the stronger nuclear potential, which implies a strong recombination amplitude and an increase in the harmonic yield. On the other hand, the stronger nuclear pull towards a single electron increases the height of the potential barrier, which decreases the probability of an electron wavefunction to tunnel through that strong barrier. This affects the ionization probability, which causes a decrease in the yield of the emitted harmonics. When we consider high ionization systems in a fixed laser field, the ionization probabilities are affected more than the recombination amplitudes, which causes a decrease in the harmonic yield of the HHG spectrum. We also observe that due to the stronger nuclear pull, small oscillations of the electron do not contribute to the HHG spectrum and quantum mechanically, only long paths participate in the HHG process. The contribution of single quantum paths in the HHG spectrum produces a supercontinuum region near the cutoff due to in-phase harmonics and this provides a suitable condition to generate single attosecond pulses from this region.

References

[1] Douhal A, Lahmani F and Zewail A H 1996 *Chem. Phys.* **207** 477
[2] Zewail A H 2000 *J. Phys. Chem. A* **104** 5660
[3] Nass K, Gorel A, Abdullah M M *et al.* 2020 *Nat. Commun.* **11** 1814
[4] Goulielmakis E, Loh Z H, Wirth A, Santra R, Rohringer N, Yakovlev V S, Zherebtsov S, Pfeifer T, Azzeer A M, Kling M F, Stephen R L and Krausz F 2010 *Nature* **466** 739
[5] Drescher M, Hentschel M, Kienberger R, Uiberacker M, Yakovlev V, Scrinzi A, Westerwalbesloh Th, Kleineberg U, Heinzmann U and Krausz F 2002 *Nature* **419** 803
[6] Pal S K and Zewail A H 2004 *Chem. Rev.* **104** 2099
[7] Uiberacker M, Uphues Th, Schultze M, Verhoef A J, Yakovlev V, Kling M F, Rauschenberger J, Kabachnik N M, Schröder H, Lezius M, Kompa K L, Muller H G, Vrakking M J J, Hendel S, Kleineberg U, Heinzmann U, Drescher M and Krausz F 2007 *Nature* **446** 627
[8] Calegari F, Trabattoni A, Palacios A, Ayuso D, Castrovilli M C, Greenwood J B, Decleva P, Martín, F and Nisoli M 2016 *J. Phys. B: At. Mol. Opt. Phys.* **49** 142001
[9] Hentschel M, Kienberger R, Spielmann C, Reider G A, Milosevic N, Brabec T, Corkum P, Heinzmann U, Drescher M, Krausz F and Schultze M 2001 *Nature* **414** 509
[10] Krausz F and Stockman, M I 2014 *Nat. Photon.* **8** 205
[11] Fabris D, Witting T, Okell W A, Walke D J, Matia-Hernando P, Henkel J, Barillot T R, Lein M, Marangos J P and Tisch J W G 2015 *Nat. Photon.* **9** 383
[12] McPherson A, Gibson G, Jara H, Johann U, Luk T S, McIntyre I A, Boyer K and Rhodes C K 1987 *J. Opt. Soc. Am. B* **4** 595

[13] Li X F, L'Huillier A, Ferray M, Lompré L A and Mainfray G 1989 *Phys. Rev. A* **39** 5751
[14] Milosevic N, Scrinzi A and Brabec T 2002 *Phys. Rev. Lett.* **88** 093905
[15] Agostini P and DiMauro L F 2004 *Rep. Prog. Phys.* **67** 813
[16] Krausz F and Ivanov M 2009 *Rev. Mod. Phys.* **81** 163
[17] Balogh E, Kovacs K, Dombi P, Fulop J A, Farkas G, Hebling J, Tosa V and Varju K 2011 *Phys. Rev. A* **84** 023806
[18] Hansen K k, Bauer D and Madsen L B 2018 *Phys. Rev. A* **67** 043424
[19] Krause J L, Schafer K J and Kulander K C 1992 *Phys. Rev. Lett.* **68** 3535
[20] Corkum P B 1993 *Phys. Rev. Lett.* **71** 1994
[21] Pfeifer T, Gallmann L, Abel M J, Neumark D M and Leone S R 2006 *Opt. Lett.* **31** 975
[22] Feng X, Gilbertson S, Mashiko H, Wang H, Khan S D, Chini M, Wu Y, Zhao K and Chang Z 2009 *Phys. Rev. Lett.* **103** 183901
[23] Feng L and Chu T 2011 *Phys. Lett. A* **375** 3641
[24] Porat G, Heyl C M, Schoun S B, Benko C, Dörre N, Corwin K L and Ye J 2018 *Nat. Photon.* **12** 387
[25] Zhai Z and Liu X 2008 *J. Phys. B: At. Mol. Opt. Phys.* **41** 125602
[26] Peng Y and Zeng H 2008 *Phys. Rev. A* **78** 033821
[27] Häffner H, Beier T, Djekić S, Hermanspahn N, Kluge H J, Quint W, Stahl S, Verdú J, Valenzuela T and Werth G 2003 *Eur. Phys. J. D* **22** 163
[28] Werth G, Alonso J, Beier T, Blaum K, Djekić S, Häffner H, Hermanspahn N, Quint W, Stahl S, Verdú J, Valenzuela T and Vogel M 2006 *Int. J. Mass Spectrometry* **251** 152
[29] Kluge H J *et al*. 2008 *Adv. Quantum Chem.* **53** 83
[30] Kraft-Bermuth S, Andrianov V, Bleile A, Echler A, Egelhof P, Grabitz P, Kilbourne C, Kiselev O, McCammon D and Scholz P 2014 *J. Low Temp. Phys.* **176** 1002
[31] Rudek B *et al*. 2013 *Phys. Rev. A* **87** 023413
[32] Young L, Kanter E, Krässig B *et al*. 2010 *Nature* **466** 56
[33] Hoener M *et al*. 2010 *Phys. Rev. Lett.* **104** 253002
[34] Abdullah M M, Anurag, Jurek Z, Son S K and Santra R 2017 *Phys. Rev. E* **96** 023205
[35] Shahbaz A, Müller C, Staudt A, Bürvenich T J and Keitel C H 2007 *Phys. Rev. Lett.* **98** 263901
[36] Shahbaz A, Bürvenich T J and Müller C 2010 *Phys. Rev. A* **82** 013418
[37] Gaarde M B and Schafer K J 2002 *Phys. Rev. A* **65** 031406
[38] Schafer K J, Gaarde M B, Heinrich A, Biegert J and Keller U 2004 *Phys. Rev. Lett.* **92** 023003
[39] Zair A, Holler M, Guandalini A, Schapper F, Biegert J, Gallmann L, Keller U, Wyatt A, Monmayrant A, Walmsley I A, Cormier, Auguste T, Caumes J P and Salieres P 2008 *Phys. Rev. Lett.* **100** 143902
[40] Hu J, Han K L and He G Z 2005 *Phys. Rev. Lett.* **95** 123001
[41] Lu R F, He H X, Guo Y H and Han K L 2009 *J. Phys. B: At. Mol. Opt. Phys.* **42** 225601
[42] Zhang H, Han K L, Zhao Y, He G Z and Lou N Q 1997 *Chem. Phys. letters* **271** 204
[43] Eberly J H, Su Q and Javanainen J 1989 *Phys. Rev. Lett.* **62** 881
[44] Burnett K, Reed V C, Cooper J and Knight P L 1992 *Phys. Rev. A* **45** 3347
[45] Gordon A, Santra R and Kärtner F X 2005 *Phys. Rev. A* **72** 063411
[46] Feng L and Chu T 2012 *J. Electron Spectrosc. Relat. Phenom.* **185** 39